ADVANCED FUNCTIONAL MATERIALS
www.afm-journal.de

A Facile and General Method for the Encapsulation of Different Types of Imaging Contrast Agents Within Micrometer-Sized Polymer Beads

*Meng-Yi Bai, Christine H. Moran, Lei Zhang, Changjun Liu, Yu Zhang, Lihong V. Wang, and Younan Xia**

Polystyrene (PS) hollow beads with holes on the surfaces are employed as containers for quick loading and encapsulation of a variety of contrast enhancement agents: saline solutions for thermoacoustic tomography, iodinated organic compounds for micro-computed tomography, and perfluorooctane for magnetic resonance. Because of the hole on the surface of the PS hollow bead, the contrast agent to be encapsulated could quickly enter the hollow interior via direct flow rather than slow diffusion through the wall. After loading, the hole on the surface is conveniently sealed by annealing the sample at a temperature (e.g., 95 °C) slightly above the glass-transition temperature of PS. In vitro methods are also used to investigate the effectiveness of encapsulation by quantifying the contrast enhancement enabled by the contrast agents.

1. Introduction

Imaging has become an indispensable tool in the fields of medicine and medical research due to many technological advances over the past 25 years.[1] Not only have new modalities been invented, such as magnetic resonance (MR) imaging, but also existing technologies have evolved, making them even more useful, as in X-ray computed tomography (CT). These developments have enabled rapid diagnosis of disease through visualization and quantitative assessment. In certain clinical applications, contrast agents are needed to locate specific lesions or organs in the body, to provide functional information, or to track the efficacy of a treatment, making many imaging modalities even more powerful. As a result, much attention is paid to the development of contrast agents for MR,[2a] ultrasound,[2b] X-ray CT,[2c] and other hybrid imaging systems such as thermoacoustic tomography (TAT).[2d]

An important aspect of contrast agent design is to minimize its potential toxicity, which can be accomplished by improving its stability in biological media and reducing the concentration necessary for effective enhancement. Encapsulating a contrast agent in a hollow particle will isolate it from the biological environment, and thus be an effective way to improve its stability regardless of the means of administration. The exterior of the hollow particle shells may also serve as a platform for surface modification, opening the door to targeted delivery and molecular imaging.

The size of particles will also impact their circulation half-life and the targeting ability, so this becomes another key design parameter. Capillaries, the smallest blood vessels, typically measure 5–10 μm in diameter. Particles used for contrast enhancement should be smaller than 5 μm in diameter to prevent capillary occlusion.[3a] However, the reticuloendothelial system (RES) will reduce the circulation half-life of particles larger than 100 nm in diameter and increase their accumulation in the liver.[3b–c] Therefore, the size of the particles should be tailored based on the particular imaging modality and target, as should the mode of delivery. For example, commercially available microbubbles for ultrasound imaging are administered by intravenous injection and their diameters are in the range of 1–5 μm, which suits the imaging needs for ultrasound applications.[3d–e]

Encapsulation by hollow colloidal particles is a process that has found widespread use in many applications such as controlled release of drugs, cosmetics, inks, chemical reagents, or biologically active species.[4] Materials frequently utilized for hollow particle synthesis include polymers,[5] lipids,[6] and proteins.[7] The two most commonly used methods for encapsulation with hollow particles are based on microemulsion[5,8] and sacrificial templating.[9] Despite their popularity, there are some disadvantages and limitations associated with these two methods. For example, the hollow particles fabricated by microemulsion usually have a broad size distribution, although

Dr. M.-Y. Bai,[+] C. H. Moran, Dr. C. Liu,[++] Y. Zhang, Prof. L. V. Wang, Prof. Y. Xia
Department of Biomedical Engineering
Washington University in St. Louis
Saint Louis, MO 63130, USA
E-mail: xia@biomed.wustl.edu
L. Zhang
Department of Medicine
Washington University Medical School
Saint Louis, MO 63110, USA
[+] Present address: Graduate Institute of Biomedical Engineering, National Taiwan University of Science and Technology, Taipei 10673, Taiwan
[++] Present address: School of Electronics and Information Engineering, Sichuan University, Chengdu 610064, China

DOI: 10.1002/adfm.201102582

optimizing the experimental parameters of emulsion processes may achieve reasonable monodispersity for the particles. In addition, the specific pairings of core and shell materials are limited, and non-uniform loading of the particles is generally observed. However, microemulsion has the major advantage of accomplishing the particle synthesis and encapsulation processes simultaneously. The particles fabricated using a sacrificial template tend to be more uniform in size, but loading the hollow core must occur after etching away the template. Therefore, the only pathway for loading relies on passive diffusion through the shell, which is not an efficient and universal solution for all types of contrast agents, especially not for macromolecules or nanoparticles.

Herein we describe a facile and generic method for preparing contrast-agent-encapsulated polymeric hollow beads with a uniform distribution of particle size. We used polystyrene (PS) beads to study contrast agent encapsulation, but biocompatible and biodegradable polymers may also be utilized.[10] The holes generated in the surface of as-prepared PS hollow beads allowed for easy loading by using reduced pressure to fill the hollow beads with a solution of a desired compound. Afterwards, the holes were sealed by annealing the system at a temperature slightly above the glass-transition temperature (T_g) of PS. These particles were then demonstrated as effective contrast agents for three different imaging modalities: MR, CT, and TAT.

2. Results and Discussion

2.1. Encapsulation of Different Contrast Agents

Figure 1 shows how to encapsulate three different types of contrast agents suitable for various imaging modalities: i) saline solutions (or NaCl microcrystals) for TAT; ii) ioversol, an iodinated contrast compound (ICC), for micro-CT; and iii) perfluorooctane (PFO) for MR imaging. These three types of contrast agents possess completely different physical properties,

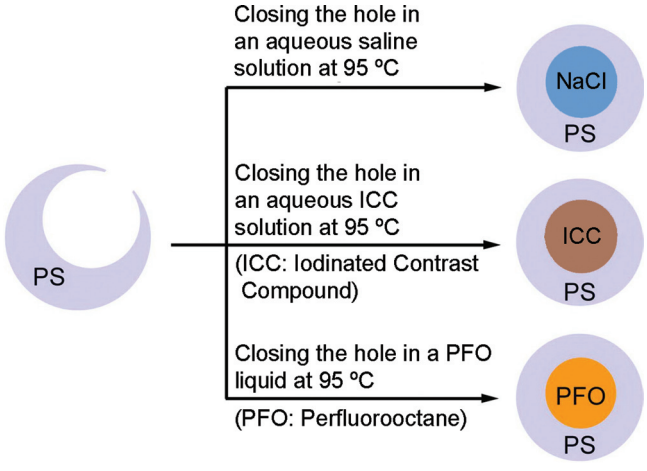

Figure 1. Schematic illustrating the procedure for closing the hole on the surface of a PS hollow bead while an imaging contrast agent is being encapsulated.

but all of them can be supplied as solutions or pure liquids for the purpose of encapsulation. Because of the high mobility of molecules in a liquid state, and the presence of a small hole on the surface of the PS hollow bead, the contrast agent quickly entered the cavity under magnetic stirring. The hole on the surface was then sealed using a thermal annealing process, encapsulating the contrast agent within the PS hollow bead.

The PS hollow beads were initially prepared with a small hole on the surface by swelling commercial PS latex beads with toluene, followed by freeze-drying, as described in previous publications.[10,11] The as-prepared PS hollow beads were then mixed with a solution (e.g., NaCl or ioversol) or a pure liquid (e.g., PFO) of the contrast agent to be encapsulated. The mixture was then subjected to the vacuum for a short period of time to induce a quick flow of the contrast agent into the cavity through the small hole on the surface. Finally, the mixture was subjected to heating at a temperature (95 °C) slightly above the T_g of PS in a capped vial to induce migration of polymer chains within each particle. As a result, the PS shell became more or less uniform in terms of thickness as the hole was closed on the surface of each PS hollow bead and a spherical cavity was generated in the interior. When the solvent evaporated during microscopy preparation, the solute (NaCl or ICC) remaining in the core of a hollow bead tended to precipitate out as a solid. Such samples could then be imaged by transmission electron microscopy (TEM) to collect direct evidence for contrast agent encapsulation. Contrast agents such as PFO that remained in a liquid state at room temperature had to be characterized using a spectroscopic method rather than TEM.

Figure 2a,b shows scanning electron microscopy (SEM) and TEM images of the as-prepared PS hollow beads with holes on their surfaces. It is clear that the solid PS beads (1.89 ± 0.03 μm in diameter and standard deviation) had been transformed into hollow beads having an average outer diameter of 2.61 ± 0.04 μm with a hole of 0.38 ± 0.04 μm on the surface. Their spherical shape and uniformity in size were both retained during the swelling and freeze-drying processes. The holes could be gradually closed by annealing the sample at a temperature (e.g., 95 °C) slightly above the T_g of PS. Figure 2c,d shows SEM and TEM images of the same batch of PS hollow beads after the sample had been annealed in water at 95 °C for 5 min. In this case, the average diameter of holes on the surfaces of PS beads was reduced from 0.38 to 0.10 μm. As shown in Figure 2e,f, the holes on the surfaces of PS beads were completely closed when the annealing time was increased to 30 min. In this case, the PS beads still had a hollow, spherical cavity in the interior while the outer diameter had been slightly reduced to 2.42 μm. Since the size of the hole in the surface can be controlled based on the choice of solvent used to swell the beads and the rate of subsequent evaporation, it is possible to make hollow beads with holes that are much larger than those used here. As shown previously, it was still possible to seal holes between 0.5–1 μm in diameter using thermal annealing or treatment with a good solvent.[10]

No polymer degradation was observed because the annealing temperature was well below the decomposition temperature of polystyrene (350–500 °C).[12] Additionally, we did not observe aggregation during the annealing process, which can be attributed to two main factors. First, a relatively low concentration

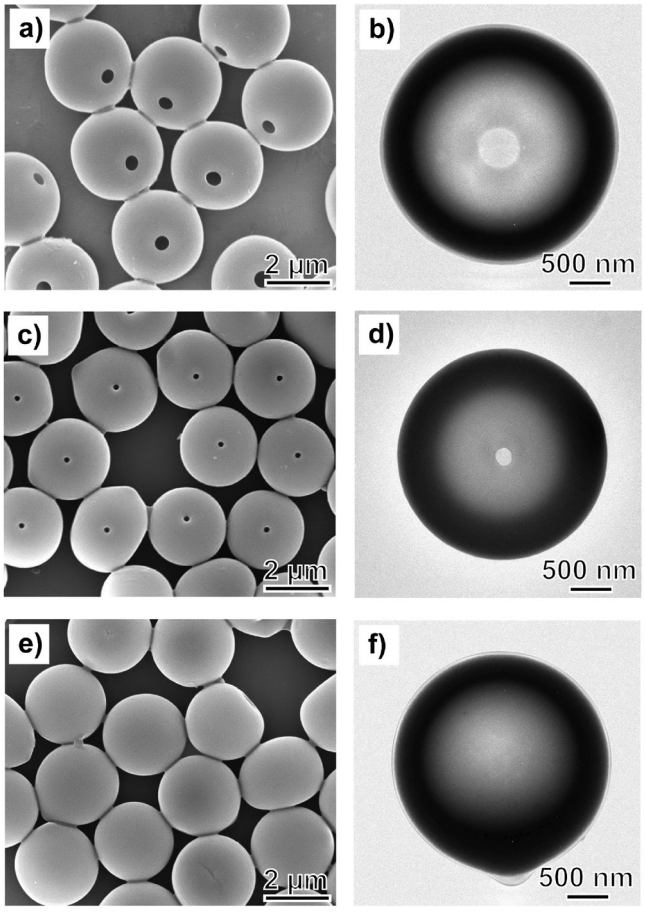

Figure 2. a) SEM and b) TEM images of the as-prepared PS hollow beads with holes on their surfaces. c) SEM and d) TEM images of the same batch of PS hollow beads where the holes had been partially closed by annealing the system in water at 95 °C for 5 min. e) SEM and f) TEM images of the same batch of PS hollow beads where the holes had been completely closed by annealing the system in water at 95 °C for 30 min.

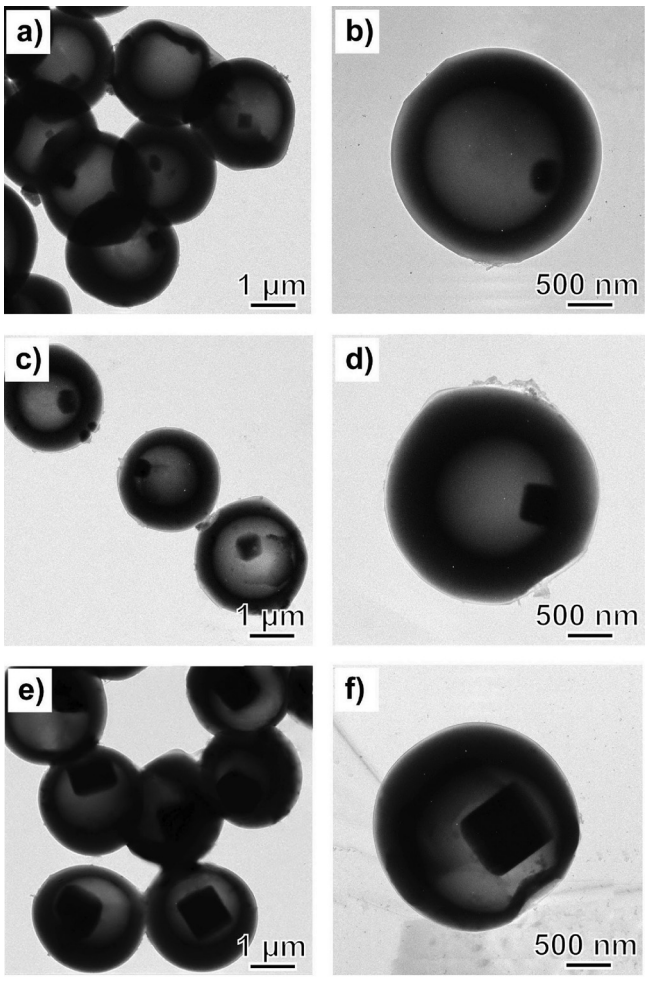

Figure 3. TEM images of the PS hollow beads that had been encapsulated with saline solutions of different concentrations: a,b) 5.9 wt%, c,d) 11.1 wt%, and e,f) 23.1 wt%. The holes were closed by annealing the samples in the corresponding saline solutions at 95 °C for 45 min. The samples were collected by centrifugation and thoroughly washed with water. The samples supported on copper grids were further dried at 75 °C for 5 min to completely remove water prior to TEM characterization.

of PS beads was used, thereby reducing the likelihood of collision and aggregation. Second, the PS beads contained negative charges from the sulfate ester used by the manufacturer. This provided an electrostatic repulsion force capable of stabilizing the PS beads, even at elevated temperatures.

We first prepared saline-encapsulated PS hollow beads to serve as a microwave-absorbing contrast agent for TAT. We simply dispersed the PS hollow beads with openings on their surfaces in saline solutions of 5.9%, 11.1%, and 23.1% (w/w) in concentration, respectively, followed by thermal annealing at 95 °C under magnetic stirring. After 45 min, the particles were collected by centrifugation and washed with deionized water to remove excess saline solution outside the hollow beads. We could only characterize samples by TEM after the water inside the hollow beads had completely evaporated. As shown in **Figure 3**, each hollow bead contained a cube-shaped NaCl microcrystal in its core. Since the samples were thoroughly washed with water prior to TEM characterization, we could rule out the possibility that the NaCl microcrystals were formed on the outer surfaces of the PS hollow beads. Interestingly, the size of the microcrystals increased as the concentration of the saline solution increased from 5.9% to 23.1%, implying that the single NaCl cube nucleated and grew from the limited supply of saline solution encapsulated in each PS hollow bead. Due to the relatively slow evaporation of water through the PS shell and the hydrophobic nature of PS, only one nucleus was formed inside each hollow bead.

We then demonstrated the feasibility of producing ICC-encapsulated PS hollow beads for use with microCT. Again, we simply dispersed the PS hollow beads with holes on their surfaces in aqueous ioversol solutions with concentrations of 25%, 51%, and 74% (w/v), respectively. The samples were then annealed at 95 °C for 45 min under magnetic stirring to close the holes on their surfaces. The products were collected by centrifugation and either suspended in water for microCT imaging or dried for characterization by TEM. Since the ICC contains a large number of iodine atoms, it had a darker contrast relative

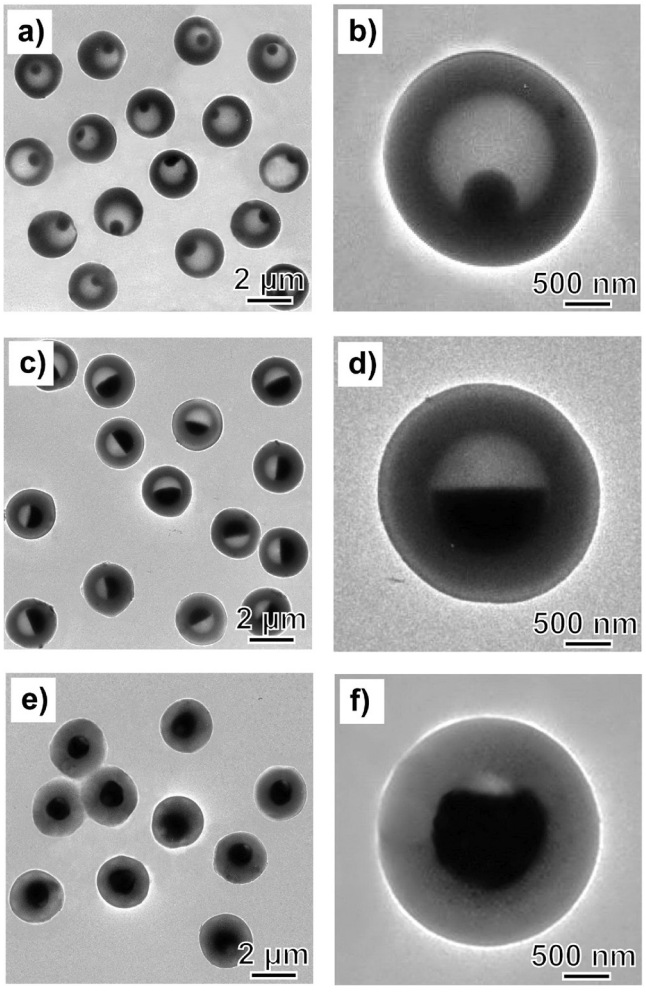

Figure 4. TEM images of PS hollow beads containing ioversol in the interiors. The holes were closed by heating the PS hollow beads at 95 °C for 45 min in aqueous solutions containing: a,b) 25%, c,d) 51%, and e,f) 74% of ioversol. The samples were collected by centrifugation and thoroughly washed with ethanol and dried at 75 °C for 5 min to completely remove the water inside the beads prior to TEM characterization.

to PS under TEM. As shown in **Figure 4**, the ICC precipitated out as a solid mass inside the core of each PS hollow bead after the water had evaporated. The volume of the solid mass also increased with the concentration of ICC in the solution used for encapsulation. When the concentration of ICC was 74%, the mass of ICC occupied nearly the entire cavity inside the PS hollow bead (Figure 4e,f).

The most appealing advantage of this method for directly loading a functional material through the holes on the surface of a PS hollow bead is that it is very straightforward and not closely tied with the properties of the material to be encapsulated. Simply mixing the PS hollow beads with a solution containing the desired material allows the solution to quickly enter into the cavity of the PS hollow beads. The original state of the desired material does not really matter as long as it can be prepared as a solution or colloidal suspension. In the aforementioned studies, we have focused on the encapsulation of two hydrophilic solids, NaCl and ICC, which can both be readily prepared as aqueous solutions. Here we further demonstrate that not only aqueous solutions but also organic liquids as hydrophobic as PFO can also be easily encapsulated in the PS hollow beads. In this case, the PS hollow beads with holes on the surfaces were dried and dispersed in PFO to obtain a homogeneous suspension. The reaction mixture was then sealed in a sample vial and placed in a 95 °C oil bath for 30 min to close the holes on the surfaces of the PS hollow beads. Since PFO is a volatile compound, the encapsulated PFO could not be observed by electron microscopy. However, the half-life of fluorine isotope ^{19}F is relatively long and has a nuclear spin of 1/2, making it easily detectable by MR spectroscopy and imaging. Specifically, ^{19}F MR spectroscopy and imaging can be performed using the same instrument used for proton MR imaging. Therefore, MR spectroscopy and imaging were used for qualitatively and quantitatively determining the encapsulation of PFO inside the cores of the PS hollow beads.

The PFO-encapsulated PS hollow beads were collected by centrifugation after the annealing process and redispersed in a centrifuge tube containing 1 mL water. 10 μL of perfluoro-crown ether (PFCE) was added into the suspension as an internal standard for the quantitative analysis. **Figure 5**a shows the ^{19}F MR spectrum acquired from this centrifuge tube containing a suspension of PFO-encapsulated PS hollow beads. As expected, two major ^{19}F peaks were detected, which were attributed to the fluorine atoms in PFO and PFCE, respectively. Since the instrument typically used for ^{1}H MR spectroscopy and imaging utilized a radiofrequency coil that was tunable to both ^{1}H and ^{19}F frequencies, we could conveniently switch back and forth to

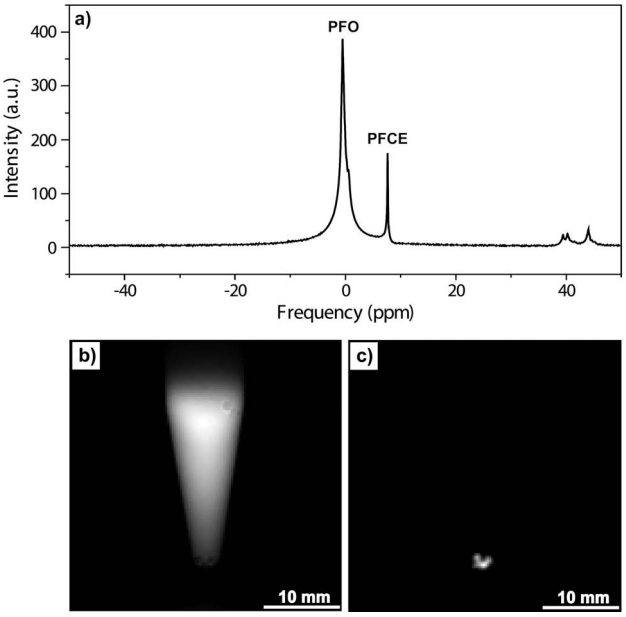

Figure 5. MR spectrum and images of PS hollow beads whose interiors had been encapsulated with PFO: a) a ^{19}F MR spectrum acquired from a sample containing PFO-encapsulated PS hollow beads and perfluoro-15-crown-5-ether (PFCE), a reference compound; b) ^{1}H mapping image from a suspension containing PFO-encapsulated PS hollow beads hosted in a centrifuge tube; and c) ^{19}F mapping image of the same sample by using the peak of PFO.

acquire spectra and images in ^{1}H or ^{19}F mode from the same sample. Therefore, the sample we used to collect the spectrum in Figure 5a was then used to acquire an image in ^{1}H mode (500 MHz) as shown in Figure 5b. We used this ^{1}H mapping image to pinpoint the position of the tube and found that the suspension appeared bright, except a very small portion at the tip of the tube. Once we switched to ^{19}F mode (470 MHz), a complementary image was observed: only the small portion at the tip of the tube was bright, but the remainder was dark (Figure 5c). Since the density of PFO (d = 1.766 g mL^{-1}) is greater than that of water, the PFO-encapsulated PS hollow beads tended to settle to the bottom of an aqueous suspension. This phenomenon explains the localization of ^{19}F signal shown in Figure 5c. We also obtained a quantitative measure of the amount of PFO presented in the sample for Figure 5a by integrating the peak area (see Supporting Information Figure S1 for detailed calculations). Three different batches of PFO-encapsulated PS hollow beads were prepared and submitted to MR quantitative analysis, respectively. The first one is shown in Figure 5a, containing 33.8 μL PFO, and the other two are shown in Figure S1 (Supporting Information), containing 33.8 and 34.2 μL PFO. The average total encapsulation of PFO measured in a typical batch of PS hollow beads was 33.9 ± 0.2 μL and each batch contained a total number of 4.6×10^{10} PS hollow beads. From the TEM image of an individual PS hollow bead, the theoretically total volume of interior cavities inside the batch of PS hollow beads was calculated to be about 33 μL (see Supporting Information Figure S2). This value is consistent with the quantitative data obtained by MR measurement. In brief, by directly loading PFO through the holes on the surfaces of PS hollow beads, we achieved high encapsulation efficiency for PFO.

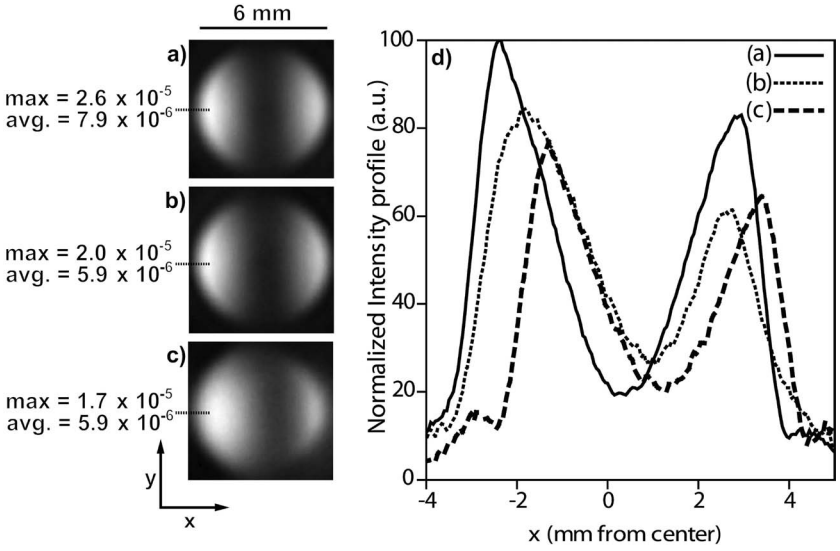

Figure 6. Thermoacoustic images of a) saline-encapsulated PS hollow beads (prepared from the 23.1% saline solution), b) DI-water-encapsulated hollow beads, and c) DI water alone contained in a 6-mm (inner diameter) LDPE tube, where "max" indicates the peak signal value in an arbitrary unit of the reconstructed image and "avg." indicates the average signal value calculated over the entire square area shown. d) Normalized signal intensity cross-section of images in (a–c), taken at the direction of the *x*-axis. Signal intensities were normalized to the peak value in (a) for saline-encapsulated hollow beads.

2.2. TAT and microCT Imaging

The saline-encapsulated PS hollow beads were evaluated as a contrast agent for TAT imaging. After annealing in the 23.1% saline solution, sealed particles were washed with water to remove excess saline solution. Samples were loaded into low-density polyethylene (LDPE) tubes at a concentration of 9.0×10^{8} particles mL^{-1}. Two control samples were imaged for comparison. The first control was deionized water alone. The second control was PS hollow beads, whose hollow interiors were filled with deionized (DI) water to confirm that the water-encapsulated PS beads did not absorb microwaves to a greater degree than water alone. **Figure 6**a–c shows the cross-sectional TAT images of all three samples. Two values were used to assess the contrast-enhancing capability of the saline-encapsulated PS hollow beads: the peak and average signals. First, the peak value of the signal was determined from the reconstructed images, where the intensities are displayed in arbitrary units. The peak intensity for saline-encapsulated PS hollow beads was 2.6×10^{-5}, which is about 1.5 times greater than deionized water alone (with a peak value of 1.7×10^{-5}). Using both the maximum and average values gives a more accurate estimate of the difference between the controls and the saline-encapsulated PS hollow beads. The average values indicate that there was virtually no difference between deionized water alone and the water-encapsulated hollow beads (5.9×10^{-6} for both samples). The average signal amplitude from the saline-encapsulated PS hollow beads was 7.9×10^{-6}, which was about 1.3 times as great as the controls.

Using microCT imaging, we evaluated the contrast enhancement ability of the ICC-encapsulated PS hollow beads. In this case, a poly(dimethyl siloxane) (PDMS) mold with a row of holes artificially created in the center was used to hold a series of aqueous suspensions of PS hollow beads encapsulating ICC solutions at different concentrations. **Figure 7**b–d shows the microCT images of a series of ICC-encapsulated PS hollow beads (all samples contained the same total number of PS hollow beads), in comparison to the blank PS hollow beads (Figure 7a). The brightness of each image was enhanced as we gradually increased the concentration of ICC used for encapsulation. The brightness of a microCT image represents the ability of the medium to absorb the incident X-ray radiation, which is quantified by the linear attenuation factor. A large attenuation factor means that the X-rays are quickly attenuated as they pass through the medium, and a small attenuation factor means that the medium is relatively transparent to X-rays. Linear attenuation factor is usually measured using units of reciprocal length. Figure 7 also shows the average values of the linear attenuation factors as a function of ICC concentration used for encapsulation. As expected, the blank PS hollow beads did not

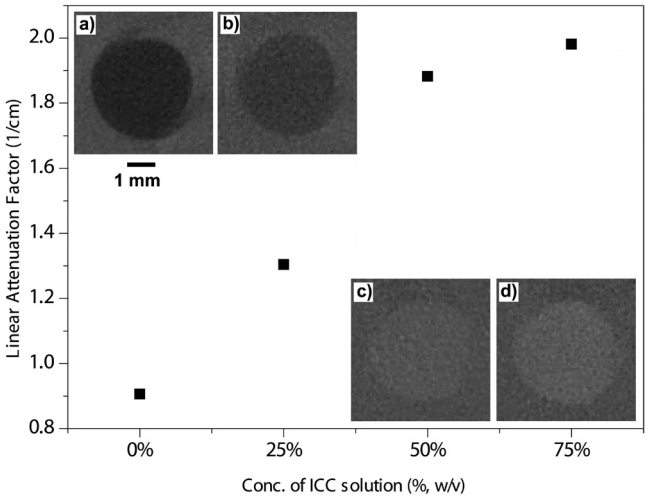

Figure 7. microCT imaging of PS hollow beads containing aqueous ICC solutions with different concentrations (used for encapsulation): a) 0%, b) 25%, c) 51%, and d) 74%. The squares shown in the figure indicate the average values of linear attenuation factors for each accompanying microCT image. The 1 mm scalebar is the same for all microCT images.

significantly attenuate X-rays. The linear attenuation factor of ICC-encapsulated beads increased as we gradually increased the concentration of ICC. In brief, the ability of ICC-encapsulated beads to attenuate X-ray radiation makes them useful as a contrast agent for CT imaging.

3. Conclusions

In summary, we have demonstrated a facile method for quick encapsulation of different types of contrast agents in PS hollow beads. As a major deviation from the emulsion method most commonly used in literature for the preparation of hollow particles encapsulated with contrast agents or drugs, we used uniform PS beads with hollow interiors and holes on the surfaces. Such hollow beads could be routinely produced in relatively large quantities by swelling commercial PS latex beads with toluene, followed by freeze-drying. The small holes on the surfaces allowed us to directly and quickly load the hollow beads with a contrast agent as long as it could be supplied as a solution or a liquid. Annealing at a temperature (e.g., 95 °C) slightly higher than the glass transition temperature of PS allowed us to close the holes and thus complete encapsulation and prevent leakage. Polymer degradation during heating was avoided by using temperatures significantly lower than the decomposition temperature of PS. Aggregation was prevented by using a relatively low concentration of PS beads for encapsulation (0.05 wt%, 0.2 wt%, and 0.4 wt% for encapsulation of saline, ICC, and PFO, respectively) and by using PS beads with negative charges on the surface.

It should be pointed out that the PS beads with micrometer-sized diameters were selected for the present work because of their availability in large quantities from commercial vendors. Other types of polymers such as poly(methyl methacrylate) (PMMA) or even those biocompatible and biodegradable such as polycaprolactone (PCL) and poly(L-lactide) have also been successfully prepared as hollow beads with openings in the surfaces and may be used for the encapsulation.[10] In addition, polymeric microspheres and nanospheres with a range of sizes may potentially be used to match the needs of particular imaging applications.

In addition to the encapsulation of contrast agents as demonstrated in the present work, this approach can also be extended to other types of chemical or biological species including drugs[13] and theranostic agents.[14] Major advantages of this new system for encapsulation include high encapsulation efficiency, good compatibility with different types of chemicals/materials, and uniformity of particle size distribution.

4. Experimental Section

Chemicals and Materials: Polystyrene (PS) latex beads of 1.89 μm in diameter were obtained from Polysciences (Warrington, PA) as an aqueous suspension (2.5% w/v or 5.68×10^9 particles mL^{-1}). Sodium chloride (99.5%), perfluorooctane (98%), and toluene (HPLC, 99.9%) were all purchased from Sigma-Aldrich (St. Louis, MO). Ioversol, an iodinated contrast compound (ICC), was obtained from Covidien (Mansfield, MA) as 51% and 74% (w/v) aqueous solutions with trade names of Optiray 240 and 350, respectively. The 25% ioversol solution was prepared by diluting the 51% solution with deionized water.

Preparation of PS Hollow Beads with a Hole on the Surface: In a typical procedure, 1 mL of the as-obtained suspension of PS latex beads was centrifuged at 10 000 rpm for 3 min. After the supernatant had been removed, the beads were redispersed in DI water (0.5 mL) to obtain a new suspension with a concentration of 5% (w/v). 0.5 mL of this suspension was added into a mixture of DI water (4 mL) and toluene (0.6 mL), followed by magnetic stirring for 1 h to allow all the toluene to diffuse into the PS beads. The suspension was then added into a liquid nitrogen bath dropwise within 2 min. Finally, the frozen mixture was placed in a freeze-drier to let toluene evaporate for 24 h, generating PS hollow beads with a hole on the surface. The final product was collected as dry powders, with a white appearance.

Encapsulation of Saline and NaCl Microcrystals: 0.125 g, 0.25 g, and 0.6 g NaCl solid was separately dissolved in 2 mL DI water to obtain saline solutions with concentrations of 5.9%, 11.1%, and 23.1%, respectively. Dried PS hollow beads (1.4 mg) were redispersed in ethanol (0.9 mL) and used as a stock solution. This stock solution (0.3 mL) was mixed with a saline solution (0.3 mL) and DI water (0.3 mL). The mixture was connected to a vacuum for 2 min, heated at 95 °C with a silicone oil bath under magnetic stirring at 60 rpm for 45 min. Afterwards, the resultant saline-encapsulated PS hollow beads (sealed, with no hole on the surface anymore) were collected by centrifugation at 9000 rpm for 15 min and washed 3 times with DI water (0.1 mL). The hollow beads were simply suspended in DI water for TAT measurements. For TEM characterization, the product was redispersed in ethanol (0.1 mL) and 5 μL of the final suspension was dropped onto a carbon-coated copper grid. The grid was put in an oven heated at 75 °C for 5 min to remove all water inside the PS hollow beads prior to TEM characterization. During the evaporation of water, the NaCl encapsulated in each hollow bead tended to precipitate out as a microcrystal.

Encapsulation of the Iodinated Contrast Compound (ICC): 3.9 mg of the dried PS hollow beads were redispersed in ethanol (1.2 mL) and used as a stock solution. This stock solution (0.3 mL) was mixed with an ioversol solution (0.3 mL, 25%, 51%, or 74% (w/v)). The suspension was connected to a vacuum for 2 min, stirred at 60 rpm at room temperature for 1 h, and then heated with a silicone oil bath at 95 °C under magnetic stirring at 60 rpm for 45 min. The resultant ICC-encapsulated PS hollow beads (sealed on the surface) were collected by centrifugation at 13 300 rpm for 3 min and washed 3 times with ethanol (0.1 mL). Finally, the product was redispersed in water (80 μL) for CT imaging. To

prepare for TEM characterization, a sample was resuspended in ethanol (50 μL), and 5 μL of the final suspension was dropped onto a carbon-coated copper grid and dried at 75 °C for 5 min to completely remove the water inside the beads.

Encapsulation of Perfluorooctane (PFO): PS hollow beads (3.8 mg) were redispersed in PFO (0.3 mL) in a centrifuge tube, and the suspension was connected to a vacuum for 2 min. Afterwards, PFO (0.2 mL) was added into the centrifuge tube to make up for the loss of PFO vaporized during vacuum. The suspension was then stirred at 60 rpm and heated at 95 °C with a silicone oil bath for 30 min. The final product was separated by centrifugation at 10 000 rpm for 3 min. The collected precipitate was kept under ambient conditions to let the PFO outside the PS beads evaporate naturally. Finally, the product was re-dispersed in water (1 mL) for magnetic resonance (MR) measurements.

Thermoacoustic Tomography (TAT): Suspensions of the saline-encapsulated PS beads (9×10^8 particles mL^{-1}, prepared from the 23.1% saline solution) were placed in low-density polyethylene (LDPE) tubes with a 6 mm inner diameter. The tubes were submerged in a mineral oil bath. Mineral oil was used as a background because it is a poor microwave absorber while being a good medium for transmitting ultrasound. A 3 GHz high-power microwave source with a 0.6-μs pulse width and a 10-Hz pulse repetition rate was applied to the bath via a standard horn antenna. The pulse power was measured to be 62 kW (37.2 mJ pulse energy). The acoustic signals generated were collected by an ultrasound transducer with a center frequency of 2.25 MHz and an active area diameter of 0.5 inch. The data were collected in a full circle around the sample, generating a cross-sectional image of the tube. Image reconstruction was performed using a delay-and-sum (backprojection) algorithm.

Micro-Computed Tomography (microCT): microCT (Scanco Medical microCT40) was used to image and characterize the ICC-encapsulated PS beads, with plain PS hollow beads serving as a control. A poly(dimethyl siloxane) (PDMS) mold with wells of 4 mm in diameter was used to hold suspensions of the PS hollow beads (80 μL $well^{-1}$). The sample was scanned at a resolution of 16 μm (45 kVp, 176 μA, and 250 ms) perpendicular to the longitudinal axis of the wells. By using the manufacturer's software (Eval v5.0), linear attenuation factors were acquired within the selected circular area (3 mm diameter) from 5 layers of each well at the same *z*-positions. Average values were presented as the final data.

Magnetic Resonance (MR): MR spectroscopy and imaging were acquired on a Varian UNITY-INOVA spectrometer (11.74 Tesla, Varian Associates, Palo Alto, CA). The PFO-encapsulated PS beads were centrifuged down to the bottom of a 1.5 mL centrifuge tube. A 2 mm tube containing 10 μL perfluoro-15-crown-5-ether (PFCE) was used as an internal standard during MR spectroscopy to enable quantification of the encapsulated PFO. MR spectroscopy and imaging were acquired using a custom-built 1-cm-diameter single-turn solenoid RF coil dual-tunable to proton and fluorine frequencies (500 MHz and 470 MHz, respectively). Water (^1H) and PFO (^{19}F) MR images were acquired with the following parameters: spin-echo sequence; TR (1s), TE (15 ms), FOV (3×3 cm^2), matrix size (128×128), in plane resolution (234×234 μm^2), thickness (10 mm), and imaging time (2 and 8.5 min, respectively).

Supporting Information

Supporting Information is available from the Wiley Online Library or from the author.

Acknowledgements

M.Y.B. and C.H.M. contributed equally to this work. This work was supported in part by an NIH Director's Pioneer Award (5DP1 OD000798) and start-up funds from Washington University in St. Louis. Part of the research was performed at the Nano Research Facility, a member of the National Nanotechnology Infrastructure Network (NNIN), which is supported by the NSF under award no. ECS-0335765. M.Y.B. acknowledges a fellowship supported by the Taiwan Merit Scholarship program (NSC-095-SAF-I-564-620-TMS).

Received: October 26, 2011
Published online: December 12, 2011

[1] C. M. C. Tempany, B. J. McNeil, *J. Am. Med. Assoc.* **2001**, *285*, 562.
[2] a) C. Sun, J. S. H. Lee, M. Zhang, *Adv. Drug Delivery Rev.* **2008**, *60*, 1252; b) J. R. Lindner, *Nat. Rev. Drug Discovery* **2004**, *3*, 527; c) A. de Vries, E. Custers, J. Lub, S. van den Bosch, K. Nicolay, H. Grüll, *Biomaterials* **2010**, *31*, 6537; d) M. Pramanik, M. Swierczewska, D. Green, B. Sitharaman, L. V. Wang, *J. Biomed. Opt.* **2009**, *14*, 034018.
[3] a) M. Anthea, J. Hopkins, C. W. McLaughlin, S. Johnson, M. Q. Warner, D. LaHart, J. D. Wright, *Human Biology and Health*, Prentice Hall, Englewood Cliffs, NJ **1993**; b) S. D. Perrault, C. Walkey, T. Jennings, H. C. Fischer, W. C. W. Chan, *Nano Lett.* **2009**, *9*, 1909; c) K.-i. Ogawara, M. Yoshida, K. Higaki, T. Kimura, K. Shiraishi, M. Nishikawa, Y. Takakura, M. Hashida, *J. Controlled Release* **1999**, *59*, 15; d) G. Schmitz, *Basic Res. Cardiol.* **2008**, *103*, 174; e) B. B. Goldberg, J.-B. Liu, F. Forsberg, *Ultrasound in Med. and Biol.* **1994**, *20*, 319.
[4] a) D. L. Wilcox, M. Berg, T. Bernat, D. Kellerman, J. K. Cochran, *Mater. Res. Soc. Symp. Proc.* **1994**, *372*, 1; b) R. Langer, *Nature* **1998**, *392*, 5; c) D. E. Bergbreiter, *Angew. Chem. Int. Ed.* **1999**, *38*, 2870; d) S. R. White, N. R. Sottos, P. H. Geubelle, J. S. Moore, M. R. Kessler, E. N. Brown, S. Viswanathan, *Nature* **2001**, *409*, 794; e) F. Caruso, *Adv. Mater.* **2001**, *13*, 11.
[5] a) G. Crotts, T. G. Park, *J. Controlled Release* **1995**, *35*, 91; b) T. Pitaksuteepong, N. M. Davies, I. G. Tucker, R. Rades, *Eur. J. Pharm. Biopharm.* **2002**, *53*, 335; c) V. Coccoli, A. Luciani, S. Orsi, V. Guarino, F. Causa, P. A. Netti, *J. Mater. Sci.: Mater. Med.* **2008**, *19*, 1703; d) T Betancourt, K Shah, L Brannon-Peppas, *J. Mater. Sci.: Mater. Med.* **2009**, *20*, 387.
[6] M. C. Woodle, *Adv. Drug Delivery Rev.* **1998**, *32*, 139.
[7] A. MaHam, Z. Tang, H. Wu, J. Wang, Y. Lin, *Small* **2009**, *5*, 1706.
[8] a) T. Freytag, A. Dashevsky, L. Tillman, G. E. Hardee, R. Bodmeier, *J. Controlled Release* **2000**, *69*, 197; b) M. F. Zambaux, F. Bonneaux, R. Gref, E. Dellacherie, C. Vigneron, *J. Controlled Release* **1999**, *60*, 179; c) S. Freitas, H. P. Merkle, B. Gander, *J. Controlled Release* **2005**, *102*, 313.
[9] a) W. Cui, J. Bei, S. Wang, G. Zhi, Y. Zhao, X. Zhou, H. Zhang, Y. Xu, *J. Biomed. Mater. Res. B: Appl. Biomater.* **2005**, *73B*, 171; b) S. Li, L. Nguyen, H. Xiong, M. Wang, T. C.-C. Hu, J.-X. She, S. M. Serkiz, G. G. Wicks, W. S. Dynan, *Nanomedicine: NBM* **2010**, *6*, 127; c) X. Yang, L. Chen, B. Huang, F. Bai, X. Yang, *Polymer* **2009**, *50*, 3556; d) G. Liu, H. Ji, X. Yang, Y. Wang, *Langmuir* **2008**, *24*, 1019.
[10] U. Jeong, S. H. Im, P. H. C. Camargo, J. H. Kim, Y. Xia, *Langmuir* **2007**, *23*, 10968.
[11] a) S. H. Im, U. Jeong, Y. Xia, *Nat. Mater.* **2005**, *4*, 671; b) M. Y. Bai, Y. Xia, *Macromol. Rapid Commun.* **2010**, *31*, 1863.
[12] T. Arii, *J. Mass Spectrom. Soc. Jpn.* **2003**, *51*, 235.
[13] L. E. V. Vlerken, M. M. Amiji, *Expert Opin. Drug Delivery* **2006**, *3*, 205.
[14] E. Pisani, N. Tsapis, B. Galaz, M. Santin, R. Berti, N. Taulier, E. Kurtisovski, O. Lucidarme, M. Ourevitch, B. T. Doan, J. C. Beloeil, B. Gillet, W. Urbach, S. L. Bridal, E. Fattal, *Adv. Funct. Mater.* **2008**, *18*, 2963.